

Evaluation of preconsolidation stress by shear wave velocity

Hyung-Koo Yoon^{1a}, Changho Lee^{1b}, Hyun-Ki Kim^{2c} and Jong-Sub Lee^{*1}

¹School of Civil, Environmental and Architectural Engineering, Korea University, Seoul 136-701, Korea

²School of Civil and Environmental Engineering, Kookmin University, Seoul 136-702, Korea

(Received June 30, 2010, Accepted August 25, 2010)

Abstract. The behaviors of saturated soils such as compressibility and permeability are distinguished by preconsolidation stress. Preconsolidation stress becomes an important design parameter in geotechnical structures. The goal of this study is to introduce a new method for the evaluation of preconsolidation stress based on the shear wave velocity at small strain, using Busan, Incheon, and Gwangyang clays in Korea. Standard consolidation tests are conducted by using an oedometer cell equipped with bender elements. The preconsolidation stresses estimated by shear wave velocity are compared with those evaluated by the Casagrande, constrained modulus, work, and logarithmic methods. The preconsolidation stresses estimated by the shear wave velocity produce very similar values to those evaluated by the Onitsuka method (one of the logarithmic methods), which yields an almost real preconsolidation stress. This study shows that the shear wave velocity method provides a reliable method for evaluating preconsolidation stress and can be used as a complementary method.

Keywords: compressibility; consolidation; fabric change; preconsolidation stress; shear wave velocity; void ratio.

1. Introduction

Consolidation tests have been commonly used to assess soil characteristics such as compressibility, permeability, and preconsolidation stress (Shang *et al.* 2009, Khan *et al.* 2010). The compressibility rate of the soils under the Ko loading condition increases at the point of preconsolidation stress, which is the maximum stress applied in the soil (Casagrande 1936). Preconsolidation stress p_c' , can be caused by loading-unloading, erosion, desiccation, secondary compression such as creep or ageing, and physico-chemical phenomena.

Many methods have been proposed for the evaluation of preconsolidation stress: Casagrande (1936), Janbu (1969), Becker *et al.* (1987), Butterfield (1979), Jose *et al.* (1989), Burland (1990), Sridharan *et al.* (1991), Onitsuka *et al.* (1995), and Wang and Frost (2004). These methods use the effective stress-void ratio relationship which reflects the global settlement without considering the small-strain behavior. On the other hand, Nagaraj and Srinivasa Murthy (1983) and Houlsby and Sharma (1999) have suggested the relationship between volumetric deformation and consolidation stress

*Corresponding Author, Associate Professor, E-mail: jongsub@korea.ac.kr

^aPost doctoral Fellow

^bResearch Professor

^cAssistant Professor

using the double-layer theory and micromechanics theory. Thus, the phenomenon of consolidation can reflect the small-strain behavior.

In this paper, a new method, namely the shear wave velocity method, is suggested for the evaluation of preconsolidation stress while considering the small-strain behavior. This paper includes a review of the commonly used methods for the preconsolidation stress evaluation, the concept of the new method, the experimental program, analyses and verification, and a conclusion.

2. Evaluation methods of preconsolidation stress

Several methods have been suggested for the evaluation of preconsolidation stress using oedometer tests under Ko loading conditions.

2.1 Casagrande method

The Casagrande method (1936) is the most commonly used method for the evaluation of preconsolidation stress. The Casagrande method is based on the void ratio e and the vertical effective stress p' in logarithmic scale as shown in Fig. 1(a). The evaluation of the preconsolidation stress p_c' is as follows: 1) in the $e - \log p'$ curve, the minimum radius of curvature is selected by visual observation; 2) the horizontal and tangential lines are drawn at the minimum radius; 3) the bisector line between the horizontal and tangential lines is drawn; 4) the tangential line is drawn from the virgin part of the arc in the $e - \log p'$ curve; 5) the intersection of the bisector line and the tangential line from the virgin part yields the preconsolidation stress. It is known that the Casagrande method is user dependent and produces 15~50% higher values than actual preconsolidation stress

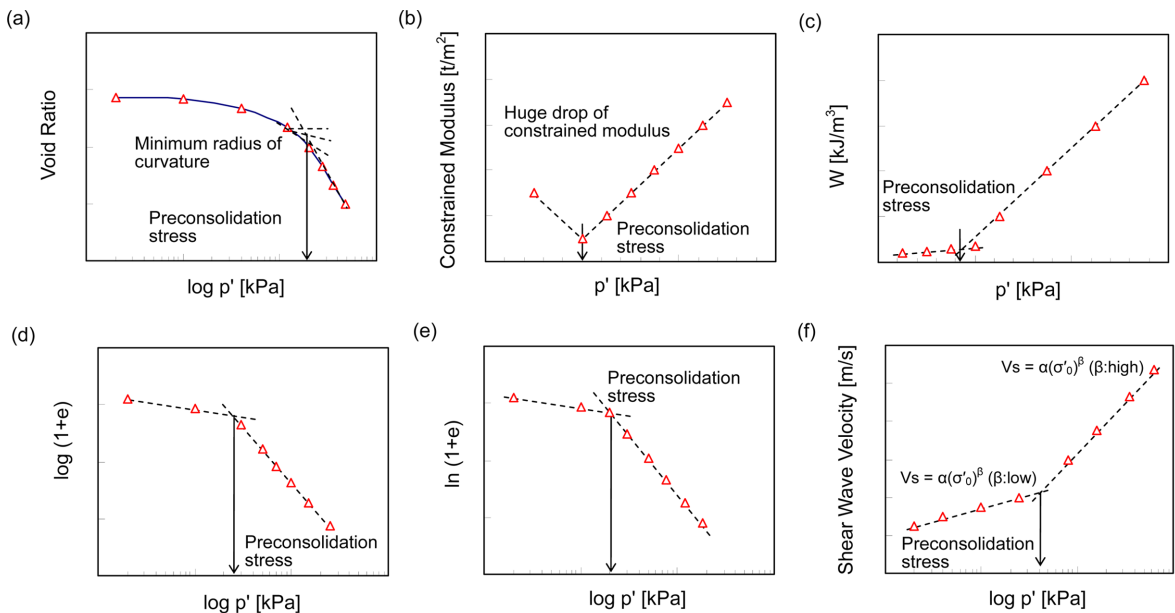


Fig. 1 Preconsolidation stress evaluation methods: (a) Casagrande, (b) Janbu, (c) Becker *et al.*, (d) Sridharan *et al.*, (e) Ontisuka *et al.*, (f) Shear wave velocity

(Jose *et al.* 1989). Because the Casagrande method uses the void ratio, which is calculated from the vertical settlement, this method is based on the global settlement.

2.2 Constrained modulus method

Janbu (1969) proposed the constrained modulus method. The constrained modulus M is the reciprocal value of the volume compressibility coefficient m_v ($M=1/m_v$). The constrained modulus M versus the effective vertical stress in arithmetic scale (M vs p') is plotted in Fig. 1(b). The significant drop of the constrained modulus due to breakdown of soil resistance stress captures the preconsolidation stress. The Janbu constrained modulus method is mainly used for high sensitive and low overconsolidation ratio (OCR) clay (Grozic *et al.* 2003). The constrained modulus is the ratio of the vertical effective stress change to the vertical strain change ($M=\Delta\sigma_v'/\Delta\varepsilon_v$) under the Ko-loading condition. Thus, this method is also based on the global settlement.

2.3 Work method

Becker *et al.* (1987) proposed the work method to improve the demarcation of preconsolidation stress. When a material is subjected to stress under the Ko-loading condition, the work per unit volume W is expressed by the stress and strain

$$\Delta W = \left(\frac{p'_{i+1} + p'_i}{2} \right) (\varepsilon_{i+1} - \varepsilon_i) \quad (1)$$

where p' and ε are the effective stress and the incremented natural strain, respectively. The subscripts i and $i+1$ refer to the loading sequences. The cumulative work per unit volume versus the vertical effective stress in arithmetic scale is plotted in Fig. 1(c) for overconsolidated clay. The cumulative work versus the effective stress is shown by the two fitted lines: one is the fitted line at the beginning of the loading part and the other is the fitted line at higher stresses. The intersection of the two lines indicates preconsolidation stress. Note that the current effective stress can also be obtained. Because the strain is based on the global settlement of the specimen, the work method also reflects global deformation.

2.4 Logarithmic methods

The logarithmic methods use the logarithmic void ratio including $\log(e)$, $\log(1+e)$, $\ln(e)$, and $\ln(1+e)$ instead of the arithmetic void ratio (e) in the void ratio versus effect stress curve ($e - \log p'$ curve). Butterfield (1979) suggested an $\ln(1+e) - \ln p'$ curve to improve the linearity of the $e - \log p'$ curve. Jose *et al.* (1989) suggested a $\log e - \log p'$ curve and Sridharan *et al.* (1991) used a $\log(1+e) - \log p'$ curve. Onitsuka *et al.* (1995) adopted an $\ln(1+e) - \log p'$ curve to avoid the negative value in the void ratio axis. All logarithmic methods can be shown by two fitted straight lines based on the lower stress portion and higher stress portion. The preconsolidation stress is the intersection of the two lines as shown in Figs. 1(d) and (e). Jose *et al.* (1989) showed that the Casagrande method produced a higher value of 15~50% for preconsolidation stress and that the $\log e - \log p'$ method yielded a 2~20% higher value for preconsolidation stress. The logarithmic method suggested by Onitsuka *et al.* (1995) can be induced from the work method, and it provided the most appropriate preconsolidation stress (Grozic *et al.* 2003). The concept of the logarithmic method is that the rate

of global settlement is higher after preconsolidation stress.

2.5 Other methods

Burland (1990) suggested the estimation method of the preconsolidation stress based on the void index, $I_v = (e - e^*_{100}) / (e^*_{100} - e^*_{1000})$, where e^*_{100} and e^*_{1000} are void ratios at $p' = 100$ kPa and $p' = 1000$ kPa, respectively. The preconsolidation stress is shown by the break in the bilinear lines of the $I_v - \log p'$ curve. Wang and Frost (2004) proposed the dissipated strain energy method to improve the linearity of the work method, which uses the accumulated total strain energy during the loading state. The dissipated strain energy method uses both unloading and reloading stages to reduce sample disturbance.

3. Shear wave velocity method

When the load or the stress is applied on saturated soils under a K_0 loading condition, an excess pore pressure is generated. As the excess pore pressure dissipates, the effective stress increases and volume change or settlement occurs. The occurrence of settlement implies a reduction in the void ratio. Note that the commonly used previous methods, which reflect the void ratio, are based on the global vertical settlement. The vertical settlement is the integration of the small vertical strain, which results in the rearrangement, rotation, and sliding of particles. The strain level of the global vertical settlement is middle or large. The small strain itself, however, was not considered in the commonly used previous methods.

Small strain behavior, rather than the integration of the small strain, can be captured by elastic waves. The elastic waves are classified according to the particle motion during wave propagation: the longitudinal wave and shear wave. The longitudinal wave propagates through soil particles and water. The shear wave, however, propagates only through soil particles. Thus, the shear waves capture the effective stress. As the particle motion in shear waves is perpendicular to the direction of wave propagation, the effective stress should be considered in two directions: the effective stress in the direction of wave propagation σ_p , and the effective stress in the direction of particle motion σ_m . The shear wave velocity in terms of the effective stresses is

$$V_s = \alpha \left(\frac{\sigma'_p + \sigma'_m}{2} \right)^\beta = \alpha (\sigma'_o)^\beta \quad (2)$$

where the α parameter and β exponent are experimentally determined, and σ'_o is the average effective stress.

As the shear waves capture the inter-particle contact behavior, the α parameter and β exponent are related to the contact behavior between the particle and packing type even at the small strain (Lee *et al.* 2005). In continuum materials, in contrast to particulate materials, the shear wave velocity is independent on the applied stresses: the α parameter is the shear wave velocity itself and the β exponent is zero. The β exponent, however, is not zero in particulate materials such as soils. Furthermore, the β exponent increases with a decrease in the density. As the β exponent is dependent on the material type (continuum, particulate, or intermediate materials), it may be related to the soil condition as well as to the effective stress.

In the overconsolidated clay, there is only a minor change in the soil fabric with an increase in the effective stress and the β exponent is a minor value or near zero value. Thus, the increment of the

shear wave velocity with the effective stress is minor, as shown in Fig. 1(f). The settlement rate with the effective stress increases dramatically if the effective stress is greater than the preconsolidation stress. The β exponent should be a higher value in the normally consolidated clays due to the severe fabric change. Thus, the slope of the $V_s - \log p'$ curve is higher in the normally consolidated region, as shown in Fig. 1(f). The inter-particle contact behavior changes dramatically at the point of preconsolidation stress because the inter-particle forces such as cementation or bonding are broken. $V_s - \log p'$ produces a bilinear curve and the intersection point of the two bilinear lines corresponds to the preconsolidation stress as shown in Fig. 1(f). At the point of preconsolidation stress, the inter-particle contact starts to break.

4. Experimental program

4.1 Specimens

A series of verification tests are carried out by using undisturbed specimens obtained at Incheon (I), Busan (B) and Kwangyang (K) in Korea as shown in Fig. 2. The undisturbed specimens were obtained by using thin-wall tubes. The dimensions of the sampler are 76.2 mm in outer diameter, 1.2 mm in wall thickness, and 820 mm in length. Table 1 shows a summary of the index properties of specimens. The specimens are obtained at the depth of 3~31 m. The natural water contents of the specimens range from 38% to 84%. The range of the specific gravity is 2.61~2.78, the range of the plastic index is 18~40%, and the unit weight ranges from 16.2 kN/m³ to 16.6 kN/m³.

4.2 Oedometer cell

The conventional oedometer cell, which is equipped with bender elements, is used to measure the settlement and bi-directional shear wave velocity simultaneously during the consolidation test. The dimensions of the brass oedometer cell are 74 mm in inner diameter, 16 mm in thickness, and 63 mm in height as shown in Fig. 3. As the thickness of the cell is thick enough, the K_0 loading condition is assumed (see details in Ko-loading in Wanatowski *et al.* 2009). The transducers are

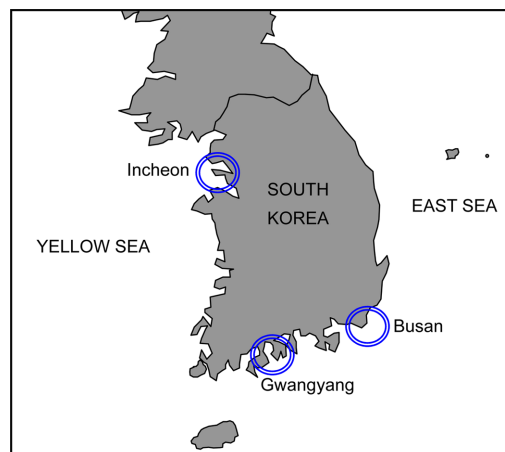


Fig. 2 Locations where specimens were obtained

Table 1 Soil properties

Sample	Depth (m)	Water content (%)	Specific gravity	Plastic limit (%)	Liquid limit (%)	Plastic index	Unit weight (kN/m ³)
Busan-A	12	62.6	2.70	26.7	56.5	29.8	16.9
Busan-B	15	58.5	2.70	27.3	53.5	26.2	17.7
Busan-C	20	70.1	2.67	28.5	68.0	39.5	17.4
Busan-D	22	72.3	2.71	31.0	72.1	41.1	17.1
Busan-E	30	51.5	2.70	24.9	52.8	27.9	16.8
Busan-F	31	49.5	2.70	26.2	55.2	29.0	18.3
Incheon-A	6	38.0	2.67	19.6	38.3	18.7	17.9
Incheon-B	6	26.3	2.58	17.1	37.3	20.2	19.3
Kwangyang-A	3	45.9	2.78	20.2	40.3	20.1	18.1
Kwangyang-B	11	84.6	2.59	42.9	71.0	28.1	15.2

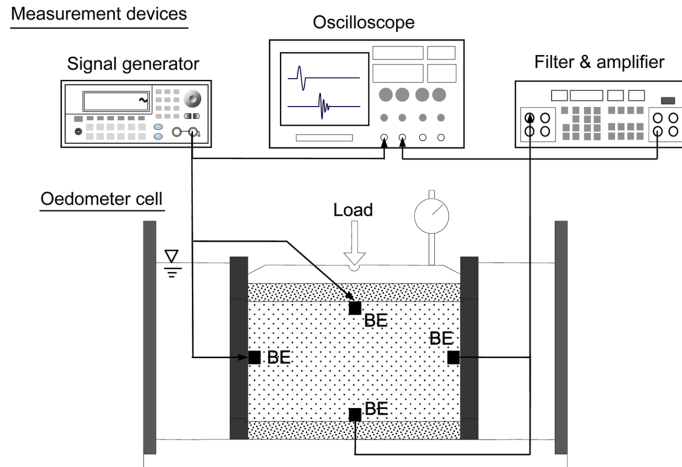


Fig. 3 Oedometer cell with bender elements and peripheral devices for measuring shear waves. The BE denotes the bender element

installed on the top cap and bottom plate for measuring vertically propagated shear waves, and they are mounted on the wall for measuring laterally propagated shear waves.

4.3 Transducers

The bender elements (Piezo Systems PSI5H4E T226-H4-Y, Parallel type), which are double-layer piezo electric materials, are used to generate and detect the shear waves. The dimensions of the bender element are 11 mm in length, 4 mm in width, 0.6 mm in thickness, and 4 mm in the cantilever length. All Bender elements are soldered to coaxial cables and coated with a thin layer of epoxy for waterproofing, and are then electrically shielded with conductive paint on the top of the epoxy layer. The conducting paint is grounded. The nylon set screws are adopted for easy installation into the oedometer cell and for the filtering of noises, including the directly transmitted waves through the cell, by using the impedance mismatch. The shear wave velocity is calculated from the travel

distance and the first arrival time. The selection of the travel distance and the travel time is based on the previous study by Lee and Santamarina (2005).

4.4 Measurement system

A single sinusoidal signal is generated by the function generator (Agilent 33220A) to produce shear waves from the source bender element. The shear wave, which propagates through the soil specimen, is detected by the receiver bender element. The measured shear waves in the form of the electrical signal are filtered and amplified through a filter-amplifier (Krohn-Hite 3364). Finally, the measured signals are digitized and stored by using an oscilloscope (Agilent 54624A) as shown in Fig. 3. The 1024 signals are stacked in order to enhance the measured shear waves.

4.5 Consolidation test

After soil specimens are placed into the oedometer cell, vertical stress is applied. The test procedure complies with ASTM D2453, which describes the one-dimensional standard consolidation testing method under the K_0 condition using incremental loading. Settlements are measured by a digital gauge with a precision of 0.001 mm. The load increment ratio is approximately 1. Each loading step lasts about 24–48 hours to ensure the dissipation of all of the excess pore pressure. When the settlement does not proceed after the dissipation of the excess pore pressure, the vertical settlement and shear waves are measured.

5. Results, analyses and verification

5.1 Results

The standard consolidation tests are carried out according to ASTM D2435. The void ratio versus the effective vertical stress in logarithmic scale for the selected specimens is plotted in

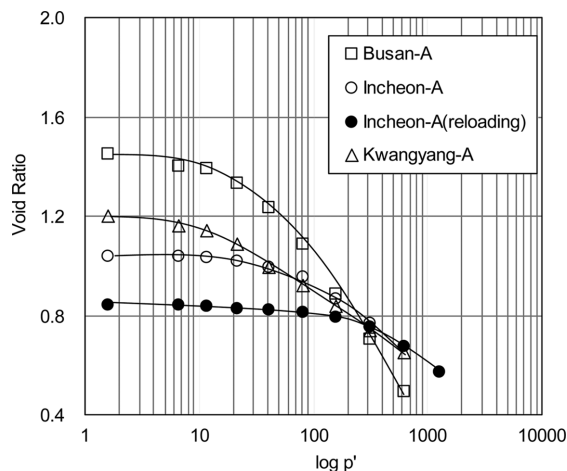


Fig. 4 e -log p' curves for the selected specimens

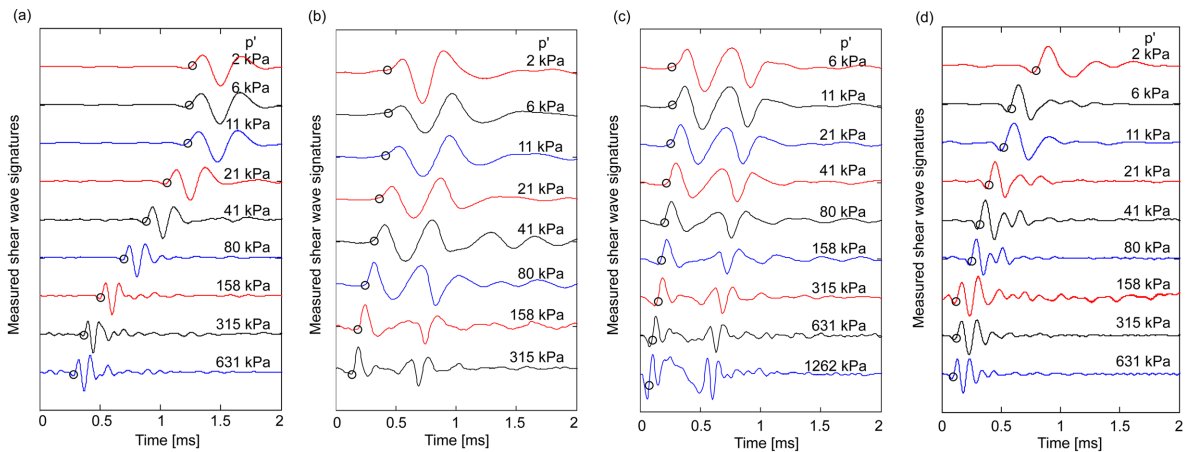


Fig. 5 Measured shear wave signatures: (a) Busan-A, (b) Incheon-A, (c) Incheon-A (reloading), (d) Kwangyang-A, the circle denotes the first arrival time

Fig. 4. The Kwangyang and Busan clays show higher compressibility than the Incheon clays. For Incheon-A clay, the vertical effective stress is applied up to 315 kPa, is maintained for 48 hours, and then removed. After unloading to zero stress, the vertical effective stress is applied up to 1260 kPa (Incheon-A - reloading). Thus, the pre-yield stress of the reloaded Incheon-A clay is about 315 kPa.

After the excess pore water pressure is fully dissipated and converted to the effective stress, the shear waves are measured. The measured shear wave signatures are plotted in Fig. 5. As the vertical effective stress increases, the first arrival time of shear waves decreases and the resonant frequency increases. The increase of the resonant frequency with the vertical effective stress reflects the increase of the stiffness (Lee *et al.* 2008).

5.2 Analyses and verification

The preconsolidation stresses evaluated by Casagrande, Janbu, Becker *et al.*, Sridharan *et al.*, Onitsuka *et al.* and the shear wave velocity method are plotted in Figs. 6~9 and summarized in Table 2 for the selected specimens. Note that Fig. 8 shows the reloading result of the Incheon-A specimen with the pre-yield stress of 315 kPa. The preconsolidation stress estimated by various methods is normalized by the Onitsuka *et al.* method, which yields the most appropriate preconsolidation stress. The normalized preconsolidation stresses are plotted in Fig. 10. Fig. 10 shows that the preconsolidation stress estimated by the Sridharan *et al.* method is nearly the same as that estimated by the Onitsuka *et al.* method because both the Sridharan *et al.* and Onitsuka *et al.* methods are basically the same logarithmic methods with a different void ratio axis. The Casagrande method estimates the preconsolidation stress at about 88~116% compared with that of the Onitsuka *et al.* method. The preconsolidation stresses evaluated by the Janbu method are about 22%~106% of the Onitsuka *et al.* method, while those evaluated by the Becker *et al.* methods are 93~160% of Onitsuka *et al.* method. Similar variations have been reported by previous researchers (Jose *et al.* 1989, Negussey and Vaid 1995, Grozic *et al.* 2003). The Janbu method extremely underestimates preconsolidation stress by approximately more than

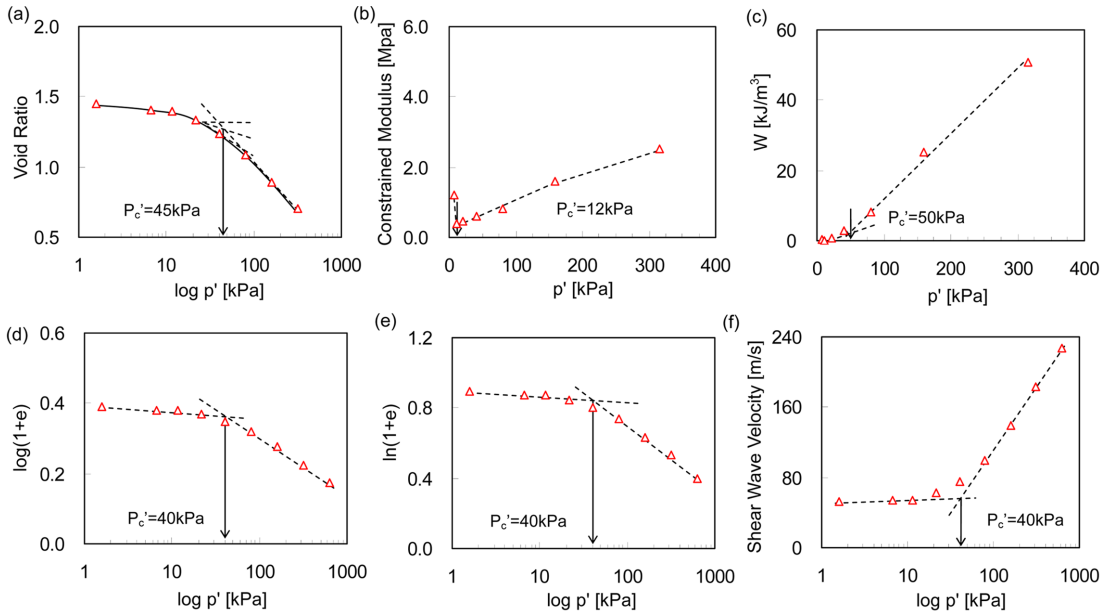


Fig. 6 Preconsolidation stress of Busan-A specimen: (a) Casagrande, (b) Janbu, (c) Becker *et al.*, (d) Sridharan *et al.*, (e) Onitsuka *et al.*, (f) Shear wave velocity

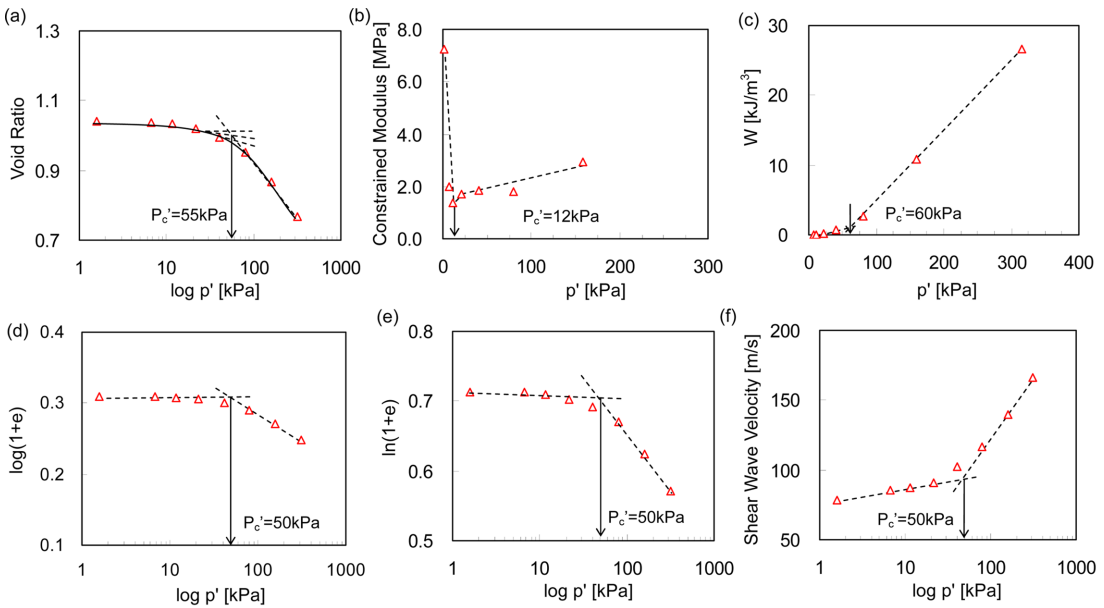


Fig. 7 Preconsolidation stress of Incheon-A specimen: (a) Casagrande, (b) Janbu, (c) Becker *et al.*, (d) Sridharan *et al.*, (e) Onitsuka *et al.*, (f) Shear wave velocity

70% because of the difficulty involved in selecting a large drop point with disturbed specimens. The preconsolidation stress estimated by the shear wave velocity method ranges from 90 to 100% of the Onitsuka *et al.* method. The results show that the new method can evaluate reliable

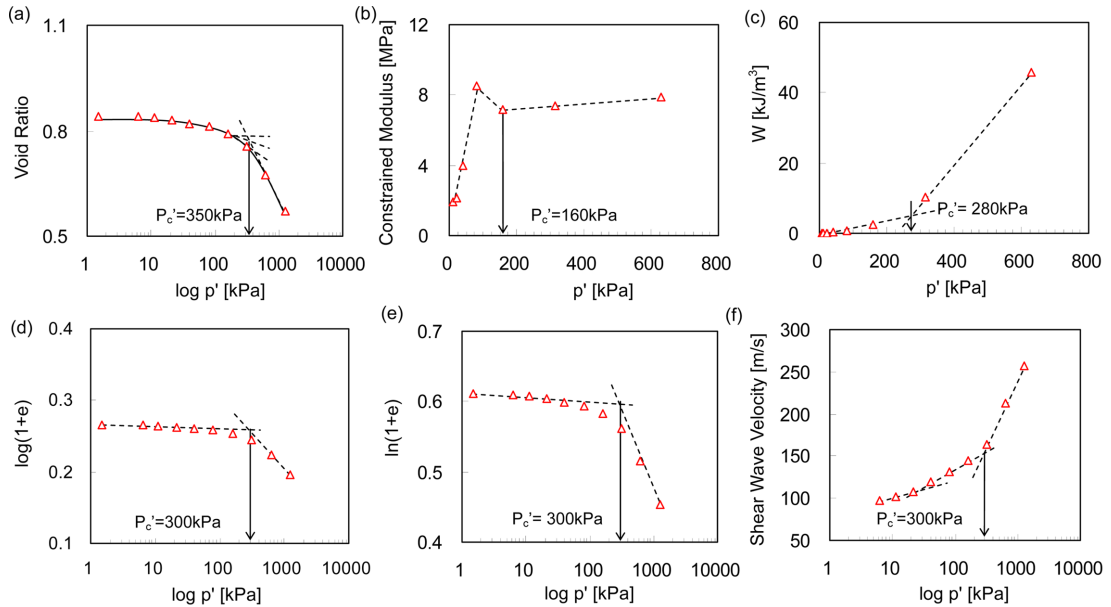


Fig. 8 Preconsolidation stress of Incheon-A reloading specimen: (a) Casagrande, (b) Janbu, (c) Becker *et al.*, (d) Sridharan *et al.*, (e) Ontisuka *et al.*, (f) Shear wave velocity

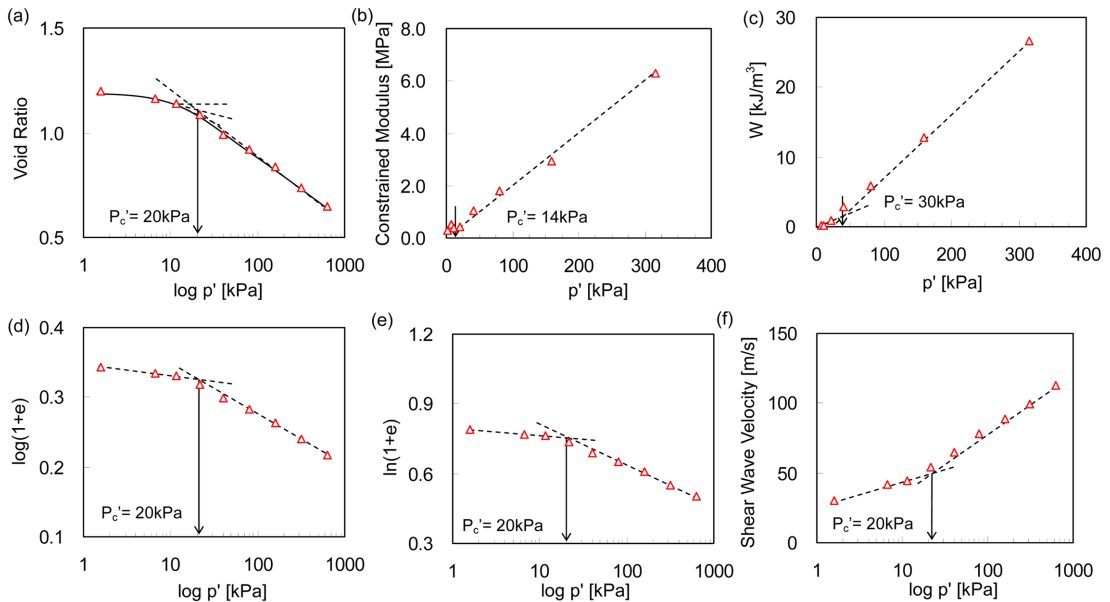


Fig. 9 Preconsolidation stress of Kwangyang-A specimen: (a) Casagrande, (b) Janbu, (c) Becker *et al.*, (d) Sridharan *et al.*, (e) Ontisuka *et al.*, (f) Shear wave velocity

preconsolidation stress. Thus, if the shear waves are measured during the conventional consolidation tests, the shear wave velocity can be used as a complementary method for the evaluation of preconsolidation stress.

Table 2 Preconsolidation stress comparison

Sample	Depth (m)	Casagrande method	Janbu method	Becker method	Sridharan method	Onitsuka method	Shear wave method
Busan-A	12	45 kPa	12 kPa	50 kPa	40 kPa	40 kPa	40kPa
Busan-B	15	30 kPa	20 kPa	30 kPa	30 kPa	30 kPa	30 kPa
Busan-C	20	55 kPa	18 kPa	80 kPa	50 kPa	50 kPa	50 kPa
Busan-D	22	105 kPa	20 kPa	110 kPa	100 kPa	100 kPa	100 kPa
Busan-E	30	90 kPa	23 kPa	90 kPa	90 kPa	90 kPa	85 kPa
Busan-F	31	100 kPa	28 kPa	100 kPa	90 kPa	90 kPa	90 kPa
Incheon-A	6	55 kPa	12 kPa	60 kPa	50 kPa	50 kPa	50 kPa
Incheon-A (reloading)	6	350 kPa	160 kPa	280 kPa	300 kPa	300 kPa	300 kPa
Incheon-B	6	40 kPa	48 kPa	50 kPa	45 kPa	45 kPa	40 kPa
Kwangyang-A	3	20 kPa	14 kPa	30 kPa	20 kPa	20 kPa	20 kPa
Kwangyang-B	11	20 kPa	10 kPa	25 kPa	20 kPa	20 kPa	20 kPa

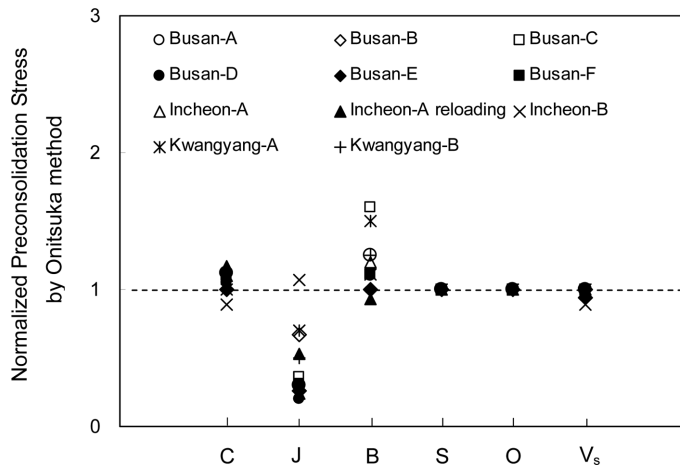


Fig. 10 Comparison of preconsolidation stresses (C: Casagrande, J: Janbu, B: Becker S: Sridharan, O: Onitsuka, and Vs: Shear wave method)

6. Conclusions

In this paper, the commonly used preconsolidation stress evaluation methods are reviewed and a new preconsolidation stress evaluation method is suggested by using shear wave velocity. Commonly used methods evaluate preconsolidation stress based on the global vertical settlement. The shear wave velocity method, however, considers the small strain, which reflects micro soil behavior. The preconsolidation stress by the shear wave velocity is the intersection point of the bilinear lines of $V_s - \log p'$. The preconsolidation stresses estimated by the shear wave velocity method produce very similar values to those evaluated by the Onitsuka method, which yields an almost actual preconsolidation stress. This study shows that the shear wave velocity is simple, easy, less time consuming and produces a reliable preconsolidation stress, and it can be used as a complementary method for the estimation of preconsolidation stress.

Acknowledgements

This work was supported by a Korea University Grant (2009) and Kookmin University Grant (2007) in Korea.

References

- ASTM D2435 (2004), "Standard test method for one-dimensional consolidation properties of soils using incremental loading", *Annual Book of ASTM Standard*.
- Becker, D.E., Crooks, J.H.A., Been, K. and Jefferies, M.G. (1987), "Work as a criterion for determining in situ and yield stresses in clays", *Can. Geotech. J.*, **24**(4), 49-564.
- Burland, J.B. (1990), "On the compressibility and shear strength of natural clays", *Geotechnique*, **40**(3), 329-378.
- Burmister, D.M. (1951), "The applications of controlled test methods in consolidation testing", *Proceedings of the Symposium on Consolidation Testing of Soils.*, Special Technical Publication.
- Butterfield, R. (1979), "A natural compression law for soils (an advance on e -log p)", *Geotechnique*, **29**(4), 469-480.
- Casagrande, A. (1936), "The determination of the pre-consolidation load and its practical significance", *Proceedings of the 1st International Soil Mechanics and Foundation Engineering Conference*, Cambridge, Mass., Ed., Casagrande.
- Grozic, J.L.H., Lunne, T. and Pande, S. (2003), "An oedometer test study on the preconsolidation stress of glaciomarine clays", *Can. Geotech. J.*, **40**(5), 857-872.
- Houlsby, G.T. and Sharma, R.S. (1999), "A conceptual model for the yielding and consolidation of clays", *Geotechnique*, **49**(4), 491-501.
- Imai, G. (1979), "Development of new consolidation test procedure using seepage force", *Soils Found.*, **19**(3), 45-60.
- Janbu, N. (1969), "The resistance concept applied to deformation of soils", *Proceedings of the 7th International Soil Mechanics and Foundation Engineering Conference*, Mexico City, A. A. Balkema, Rotterdam.
- Jose, B.T., Sridharan, A. and Abraham, B.M. (1989), "Log-log method for determination of preconsolidation pressure", *Geotech. Testing J. ASTM*, **12**(3), 230-237.
- Khan, P.A, Madhav, M.R. and Reddy, E.S. (2010), "Consolidation of thick clay layer by radial flow non-linear theory", *Geomech. Eng.*, **2**(2), 157-160.
- Kwon, T.H. and Cho, G.C. (2005), "Smart geophysical characterization of particulate materials in a laboratory", *Smart Struct. Syst.*, **1**(2), 217-233.
- Lee, C., Lee, J.S., Lee, W. and Cho, T.H. (2008), "Experiment setup for shear wave and electrical resistance measurements in an oedometer", *Geotech. Test. J.*, **31**(2), 149-156.
- Lee, J.S. and Santamarina, J.C., (2005), "Bender elements: performance and signal interpretation", *J. Geotech. Geoenviron.*, **131**(9), 1063-1070.
- Lee, J.S., Fernandez, A.L. and Santamarina, J.C. (2005), "S-wave velocity tomography: small-scale laboratory application." *Geotech. Test. J.*, **28**(4), 336-344.
- Nagaraj, T.S. and Srinivasa Murthy, B.R. (1983), "Rationalization of Skempton's compressibility equation", *Geotechnique*, **33**(4), 433-443.
- Negussey, D. and Vaid, Y.P. (1995), "Estimating maximum past pressures in clay", *Proceedings of the International Symposium on Compression and Consolidation of Clayey soils*, Hiroshima.
- Onitsuka, K., Hong, Z., Hara, Y. and Yoshitake, S. (1995), "Interpretation of oedometer test data for natural clays", *Soils Found.*, **35**(3), 61-70.
- Schmertmann, J.H. (1955), "The undisturbed consolidation behavior of clay", *TAS Civil Engineers*, **20**, 1201-1233.
- Shang, J.Q., Tang, Q.H. and Xu, Y.Q. (2009), "Consolidation of marine clay using electrical vertical drains", *Geomech. Eng.* **1**(4), 275-289.
- Sridharan, A., Abraham, B.M. and Jose, B.T. (1991), "Improved technique for estimation of preconsolidation

- pressure”, *Geotechnique*, **41**(2), 263-268.
- Wanatowski, D., Chu, J. and Gan, C.L. (2009), “Compressibility of Changi sand in K0 consolidation”, *Geomech. Eng.*, **1**(3), 241-257.
- Wang, L.B. and Frost, J.D. (2004), “Dissipated strain energy method for determining preconsolidation pressure”, *Can. Geotech. J.*, **41**(4), 760-768.
- Zeng, X. (2006), “Applications of piezoelectric sensors in geotechnical engineering”, *Smart Struct. Syst.*, **2**(3), 237-251.